PARTICULATE FOULING DURING BOILING AND NON-BOILING HEAT TRANSFER

H. Müller-Steinhagen, F. Reif, N. Epstein, A.P. Watkinson
Dept. of Chemical Engineering, University of British Columbia
Vancouver B.C., Canada V6T 1W5

ABSTRACT

Heat transfer fouling of 2 μm alumina particles suspended in heptane was investigated experimentally with an internally heated rod in an annulus and a coiled wire mounted in crossflow. Flow velocity, bulk temperature, heat flux, system pressure and particle concentration were varied over a wide range. The operating conditions included both laminar and turbulent flow with boiling and non-boiling heat transfer.

With few exceptions, all runs were continued until an asymptotic fouling resistance was reached. The value of this resistance increased with increasing particle concentration and decreasing bulk temperature. It showed maxima at certain values of the flow rate for fixed values of the heat flux and for certain values of the heat flux for fixed values of the flow rate. If the initial surface temperature was kept constant the asymptotic fouling resistance decreased continously with increasing flow rate. For many experiments, the fouling resistance measured on the coiled wire probe seemed to be less affected by changes in the hydrodynamic and thermal conditions than that on the annular flow assembly.

1. INTRODUCTION

Although much useful fouling work has been done in the last twenty years [1], the necessity to add crudely estimated fouling resistances [2] to account for the undesired deposition of material on heat exchange surfaces continues to undermine the usefulness of sophisticated methods for evaluating the heat transfer coefficients of clean heat exchangers. Therefore more basic research must be done on the various mechanisms of fouling to enable the prediction of fouling rates.

One of the major categories of fouling [1,3] involves the deposition of particles originally suspended in the fluid onto the heat exchange surface. These particles may consist of corrosion products (e.g. Fe_2O_3, Fe_3O_4), chemical reaction products (e.g. polymers) or dirt (e.g. clay, sand).

Models describing fouling usually are based on the well-known concept of Kern and Seaton [4] that the growth of the deposit at the wall is the net result of a deposition and a removal process.

$$dm/dt = \dot{m}_d - \dot{m}_r \qquad (1)$$

In integrated form, eq.(1) may be written as

$$R_f = R_f^* \left\{1 - \exp(-t/t_c)\right\} \qquad (2)$$

The initial fouling rate, which according to this model is equal to the gross deposition rate throughout the run, is then

$$\left(\frac{dR_f}{dt}\right)_{t=0} = \frac{R_f^*}{t_c} \qquad (3)$$

For particulate fouling, the deposition term in eq.(1) is usually calculated as a particle diffusion process [4,5] or via a stopping distance model [6,7,8]. It is noteworthy that the latter models are mainly based on experiments with particles in gas streams and have not in general been confirmed for liquids [8]. The removal term was introduced as a function of the wall shear stress and the deposit thickness to account for the frequently observed asymptotic behaviour of the fouling curves. However, several authors [9,10] reject the universality of particle removal and claim that other mechanisms, such as crevice corrosion and electrical double layer effects, are responsible in certain instances for the decreasing fouling rates as fouling proceeds.

There is also a definite lack of experimental evidence concerning the possible effects of heat flux, wall temperature, heat transfer mode (boiling or non-boiling) and bulk temperature on particulate fouling rates. Therefore extensive measurements with alumina particles suspended in n-heptane were performed over the range of parameters given in Table 1.

2. DESCRIPTION OF TEST EQUIPMENT

Two previously studied fouling probes [11], namely, a heated rod in an annulus and a coiled wire in cross-flow, were used. Some changes were made in the circuit to improve thermal stability and to allow visual observation of the heated sections. Some details on the construction of the heating elements are given in Table 2. The two test sections are mounted in parallel to measure simultaneously the heat transfer from the cylindrical rod and from the coiled wire (Fig. 1). The fluid is pumped from the supply tank via orifice meters to the probes. Due to the high fluid velocity, no particle deposition took place in the orifices and the pressure drop over the flow meters remained constant during each run. Fluid samples could be taken at two locations. The difference in concentration between the two locations was found to be negligible. The particle concentration was evaluated by passing a sample of the suspension through a 0.3 μm micropore glass filter.

The electrically heated stainless steel coil, or 'hot wire probe', was mounted normal to the flow in a rectangular duct. The heat flux supplied by the wire was calculated from the measured current and voltage. The wire temperature could be determined by the change of electrical resistance with wire temperature. To obtain reproducible values of the wire temperature the coil was heated several days in a vacuum oven before using. Despite this conditioning procedure, considerable scatter of the measured temperatures could not be avoided at low heat fluxes ($\dot{q} < 5000$

W/m^2), as the accuracy limit of the data logger was then reached. The bulk temperature around the hot wire probe was determined by two thermocouples located 19 mm upstream and downstream, respectively, from the coil.

The probe for the annular flow assembly was supplied by Heat Transfer Research Inc. [12]. It consisted of a stainless steel sheathed resistance heater with four thermocouples located close to the heating surface. The bulk temperature was measured with thermocouples located in mixing chambers before and after the annulus.

3. DATA REDUCTION

The experimental results are given in terms of fouling resistance versus time curves. The fouling resistance R_f was calculated from

$$R_f = \frac{T_w - T_{w,o}}{\dot{q}} \qquad (4)$$

where $T_{w,0}$ and T_w are the wall temperatures at times t=0 and t=t, respectively. This equation implies that the heat transfer coefficients and the heat transfer area remain constant throughout the fouling run. As some of the effects caused by changes in the thermal and hydrodynamic conditions due to the growing fouling deposit cancel each other and as it is not possible to evaluate these secondary effects with great accuracy, the above simplifications were accepted.

The experimental evaluation of the wall temperature and the heat flux for both the annular probe and the hot wire is described in [13]. For evaluating the clean wall temperature, $T_{w,0}$, it is customary to use the first measured temperatures of a fouling run. However, since the fouling rates at the beginning of the present experiments were found to be rather high, the value of $T_{w,0}$ was calculated instead using recommended correlations [13] for convective sensible heat transfer and subcooled boiling heat transfer.

4. TEST MATERIALS

Aluminum oxide particles (Microlux-RZ, A. Meller Company) suspended in heptane were chosen because this combination offers a number of advantages:

1. The system is chemically inert, i.e., there are no additional mechanisms affecting the fouling, such as corrosion or other chemical reactions.
2. A direct comparison with measurements for polymerization fouling [11] of heptane-styrene mixtures is possible.
3. The Al_2O_3 particles show no tendency to form large agglomerates and are readily available at a reasonable price.
4. Aluminum oxide has a comparatively low thermal conductivity and therefore yields a clear increase in the wall temperature even for thin fouling layers.

The size distribution of the particles in the suspension was evaluated several times throughout the experiments. The analyses

were performed using an electron microscope in conjunction with a particle size analyzer (Leitz image analyzer). Fig. 2 shows a typical size distribution of suspended particles. Generally, an arithmetic mean diameter between 1.5 μm and 2.5 μm was found. Thus, the average diameter of the particles was taken to be 2 μm.

5. EXPERIMENTAL RESULTS

5.1 General Observations

Figures 3a and 3b show typical results of the fouling resistance plotted as a function of time for the annular probe and the coiled wire, respectively. In all the experiments, fouling started without an induction period, which is in accordance with other particulate fouling investigations [3,5,14]. Asymptotic behaviour was found for almost every run. The duration of the runs varied from several hours to several days. The maximum asymptotic fouling resistance measured was about 5.8 m^2K/kW. From photographs taken during the experiments this resistance was attributed to a fouling layer of approximately 2 mm thickness on the annular probe. Figure 4 shows the annular probe covered with a thick deposit. The arrow marks the beginning of the heated section, where a change in deposit thickness and consistency may be observed. Generally, the fouling layer was considerably thinner than in Figure 4 and showed a very smooth surface. For the coiled wire, no photographs could be taken during the experiments due to deficient light conditions. From the deposit thickness and the corresponding fouling resistance the thermal conductivity of the layer was calculated

to be 0.35 W/mK. As the thermal conductivity of heptane is 0.14 W/mK and of Al_2O_3 3.414 W/mK, this value suggests that the deposit consists of a loosely packed layer of particle agglomerates. Attempts to measure the layer thickness with a micrometer failed, as even the most careful reduction of the liquid level in the annulus resulted in a removal of considerable amounts of the deposit.

Although the time dependence of the fouling resistance agreed fairly well with the shape predicted by eq. (2), it was usually not possible to obtain an accurate curve-fit of both the high initial fouling rate and the asymptotic fouling resistance with one set of parameters. The same curve-fitting difficulty was found by Newson et al. [14] for magnetite deposition from water suspensions. Therefore, R_f^* was determined by curve-fitting the complete fouling run to eq. (2), while for the evaluation of the initial fouling rates only the data of the first thirty minutes were used.

5.2 Comparison of Annular Probe and Hot Wire Probe

In general, both probes qualitatively showed the same influence of the parameters $\dot{m}$, $\dot{q}$, T_b and C on the fouling process. However, the coiled wire was often found to be less affected by changes in the thermal and hydrodynamic conditions than the annular probe. While the fouling resistance versus time plots mostly had a smooth shape for the measurements in the annulus, 'saw tooth' behaviour was rather common for the

measurements with the coiled wire (Fig. 5). Apparently parts of the deposit broke off as soon as a certain thickness was reached.

A fouling resistance of 2.4 m^2K/kW was found to be the limiting value for the coil, whereas fouling resistances up to 5.8 m^2K/kW were measured for the annular probe. It may be reasoned that the thin wire can give less support to the deposit because of its vastly different dimensions and configuration.

5.3 Influence of the Particle Concentration

Of all the investigated parameters, the particle concentration showed the strongest influence on the fouling process. As is evident from Figures 3a and 3b, more extensive and rapid fouling occurs on both probes as the concentration is increased. Figures 6a and 6b show the asymptotic fouling resistance as a function of the particle concentration for the annular probe and the coiled wire, respectivly. For both probes, the asymptotic fouling resistance increases roughly linearly with increasing particle concentration. However, while this increase already starts at the lowest concentrations for the coil, a minimum particle concentration seems to be necessary to initiate fouling on the annular probe. The latter result, which may be attributed to the much higher flow velocities in the annulus, was also found for hematite particles in water by Hopkins [10], who could not detect any deposition on the inside of a tube for particle concentrations below 2000 ppm. Figures 6a and 6b illustrate that under typical conditions the annular probe

generally gives higher asymptotic fouling resistances than the coiled wire.

Attempts were made to evaluate the fouling rates at the beginning of the experiments as a function of the various operating parameters. However, as the deposition was found to occur very quickly at the beginning, the scatter of the data in this region makes the evaluation of initial fouling rates difficult and uncertain. Figure 7a shows the initial fouling rate for the annular probe as a function of the particle concentration for three different bulk temperatures. Despite the scatter of data one can see that the initial rate increases linearly with the particle concentration. A different result is obtained from Figure 7b, which shows the initial fouling rates for the coiled wire as a function of the particle concentration and the mass velocity. Although there are few data points at concentrations below 50 ppm, the influence of the particle concentration appears to be much stronger, the initial deposition rate varying with the concentration to a power of about 2.3. An explanation for this behaviour cannot be given. However, it was observed that due to the low flow velocities past the coiled wire large particles tended to accumulate in the channel around the wire. Therefore, the particle concentration in the channel may have been somewhat different from that in the rest of the loop.

5.4 Influence of the Flow Velocity

Figures 8a and 8b show the influence of the flow velocity on the asymptotic fouling resistance for the flow in the annulus and past the coiled wire, respectively. Both diagrams contain two sets of data, one measured with a constant heat flux, the other measured with a constant initial wall temperature. While the asymptotic fouling resistance decreases continuously with increasing velocity if the initial wall temperature is the same for each run, it shows a distinct maximum if all runs are done with the same heat flux. This result holds for both probes. It is therefore obvious that the wall temperature (and hence the heat flux) is an important parameter.

Figure 7b shows the initial fouling rates for the coiled wire as a function of the particle concentration for various flow velocities. Within the investigated range, no influence of the flow velocity was found. A similar result was obtained for the flow in the annulus.

5.5 Influence of the Heat Flux

The influence of the heat flux on the asymptotic fouling resistance is demonstrated in Figure 9. For both probes, the heat flux was varied from 0 W/m^2 to 375,000 W/m^2 at constant system pressure, flow velocity, bulk temperature and particle concentration. For the measurements with zero heat flux (shown in the semilog plot at 20 W/m^2) both probes were heated every six hours for a few minutes. The asymptotic fouling resistance has a

maximum for the annular probe and for the coiled wire at heat fluxes of 11,000 W/m² and 25,000 W/m², respectively. Increasing the heat flux past the maximum leads to a sharp decrease of the asymptotic fouling resistance, which finally goes to zero for the highest heat fluxes. It is worthy of note that the maximum fouling resistance for both heaters occurs at an initial surface temperature of approximately 46°C.

In experiments with already fouled surfaces it was observed that the deposit was literally blown off if the heat flux was increased to very high values. It may be concluded that the attachment of the particles to the wall is then prevented by the bubble activity for developed subcooled boiling. This behaviour was observed during the initial experiments. Several tests showed that no difference existed in heat transfer and fouling behaviour between experiments where the probe was initially wiped clean and experiments where it was 'cleaned' by heating with the highest possible heat flux. As the latter method is much more convenient because it can be done without stopping and dismantling the set-up, it was used to clean the surface throughout the subsequent experiments.

For the conditions given in Figure 9, boiling started in the annulus for $\dot{q}$ = 45,000 W/m² and at the coiled wire for $\dot{q}$ = 90,000 W/m². However, the decline of the asymptotic fouling resistance was observed at heat fluxes well below these values. Therefore, other mechanisms in addition to bubbling have to be responsible for the observed trends. One possible explanation

could be the contribution of thermophoretic forces directed away from the heating surface and increasing with increasing heat flux [15]. If this hypothesis is correct, the heat flux should not only influence the values of the asymptotic fouling resistance but also have a noticeable effect on the initial fouling rates, which are assumed to be a measure of the gross deposition rates. As a matter of fact, it was found that for the measurements with the coiled wire the initial fouling rates start to decrease if a heat flux of 70,000 W/m^2 was exceeded. For the highest heat flux (375,000 W/m^2), the deposition rate was equal to zero.

For runs with high particle concentration, i.e. thick fouling deposits, tiny chimneys were observed in the deposit, which allowed for evaporation if the temperature at the surface of the heating elements exceeded the saturation temperature of the heptane. Similar boiling chimneys have been described by Macbeth [16]. The number of these chimneys increased with increasing heat flux, thus making the deposit more porous and more susceptible to break-off.

5.6 Influence of the Bulk Temperature

Although no reasonable explanation for the effect has been proposed [3], the bulk temperature had a considerable influence on the asymptotic fouling resistance - Figure 10. The dashed line in this figure represents the data for a bulk temperature of 30°C, as shown in Figure 6a. While an increase of the bulk temperature from 30°C to 50°C had no effect at all, a reduction

of the bulk temperature from 30°C to 20°C resulted in a remarkable increase of the asymptotic fouling resistance. For higher flow velocities, this increase was even more pronounced. It was observed that the deposit for the runs with the low bulk temperature was very porous and broke off easily. As Figure 7a shows, the bulk temperature has no influence on the initial fouling rates. Appearently, then, the bulk temperature mainly affects the structure of the deposit.

5.7 Influence of the System Pressure

As may be expected, the system pressure had no influence on the fouling rates as long as heat was transferred by convection. If, for a given heat flux, boiling was induced by decreasing the system pressure, a considerable decrease of the deposition rate was noted, presumably due to the repelling action of the bubbles.

6. NOMENCLATURE

C	ppm	particle concentration
m	kg/m^2	mass of deposit per surface area
$\dot{m}$	kg/m^2s	mass velocity of heptane
$\dot{m}_d$	kg/m^2s	deposition flux
$\dot{m}_r$	kg/m^2s	removal flux
p	bar	pressure
$\dot{q}$	W/m^2	heat flux
R_f	m^2K/W	fouling resistance
R_f^+	m^2K/W	asymptotic fouling resistance

t	min	time
t_c	min	time constant
T_b	°C	bulk temperature
T_w	°C	wall temperature
$T_{w,0}$	°C	initial wall temperature
u	m/s	flow velocity

7. ACKNOWLEDGEMENTS

The authors are indebted to the German Research Council (DFG) and the Ernest-Solvay-Foundation for financing the fellowships of H. Müller-Steinhagen and F. Reif, respectively. The continuing financial support of the Natural Sciences and Engineering Research Council of Canada is gratefully acknowledged.

8. REFERENCES

1. Epstein,N., Thinking about Heat Transfer Fouling : A 5x5 Matrix, Heat Transfer Engineering, vol. 4, no. 1, pp. 43-56, 1983.
2. Standards of the Tubular Exchanger Manufacturers Association (TEMA) 6th ed., pp.140-142, TEMA, New York, 1978.
3. Somerscales,E.F.C. and Knudsen,J.G., Fouling of Heat Transfer Equipment, Hemisphere Publ. Corp., Washington, 1981.
4. Kern,D.Q. and Seaton,R.E., A Theoretical Analysis of Thermal Surface Fouling, Br. Chem. Eng., vol. 4, no. 5, pp.258-262, 1959.
5. Watkinson,A.P. and Epstein, N., Particulate Fouling of

Sensible Heat Exchangers, Proc. 4th. Int. Heat Transf. Conf., vol. 1, paper HE 1.6, 1970.

6. Friedlander,S.K. and Johnstone,H.F., Deposition of Suspended Particles from Turbulent Gas Streams, Ind. Eng. Chem., vol. 49, no. 7, pp. 1151-1156, 1957.
7. Beal,S.K., Deposition of Particles in Turbulent Flow on Channel or Pipe Walls, Nuclear Science and Engineering, vol. 40, pp.1-11, 1970.
8. Papavergos,P.G. and Hedley,A.B., Particle Deposition Behaviour from Turbulent Flows, Chem. Eng. Res. Des., vol. 62, pp. 275-295, 1984.
9. Thomas,D. and Grigull,U., Experimental Investigation of the Deposition of Suspended Magnetite from the Fluid Flow in Steam Generating Boiler Tubes, Brennstoff-Wärme-Kraft, vol.26, no. 3, pp. 109-117, 1974.
10. Hopkins,R.M. and Epstein, N., Fouling of Heated Stainless Steel Tubes With Ferric Oxide From Flowing Water Suspensions, Proc. 5th Int. Heat Transf. Conf., vol. 2, pp.180-184, 1974.
11. Fetissoff,P.E., Watkinson, A.P. and Epstein, N., Comparison of Two Fouling Probes, Proc. 7th. Int. Heat Transf. Conf., vol. 6, pp. 391-396, 1982.
12. Fischer,P., Suitor,J.W. and Ritter,R.B., Fouling Measurement Techniques, Chem. Eng. Prog., vol. 71, no. 7, pp. 67-72, 1975.
13. Müller-Steinhagen,H., Watkinson,A.P. and Epstein,N., Subcooled Boiling Heat Transfer to Heptane Flowing Inside an Annulus and Past a Coiled Wire, ASME paper HTD-vol. 47,

pp.161-165, 1985.

14. Newson, I.H., Bott, T.R. and Hussain, C.I., Studies of Magnetite Deposition From a Flowing Suspension, Chem. Eng. Commun., vol. 20., pp. 335-353, 1983.

15. Whitmore,P.F. and Meisen,A., Estimation of Thermo- and Diffusiophoretic Particle Deposition, Can. J. of Chem. Eng. vol. 55, pp. 279-285, 1977.

16. Macbeth, R.V., Fouling in Boiling Water Systems, chapter 15 of Two-Phase Flow and Heat Transfer, D. Butterworth and G.F. Hewitt, eds., Oxford Univ. Press, 1977.

FIGURES

Fig. 1 Test loop.

Fig. 2 Typical size distribution for suspended particles.

Fig. 3 Fouling resistance vs. time for flow in the annulus and past the coiled wire: effect of particle concentration.

Fig. 4 Annular probe with deposit.

Fig. 5 Fouling resistance vs. time for flow in the annulus and past the coiled wire.

Fig. 6 Asymptotic fouling resistance as a function of the particle concentration for the annular probe (a) and for the coiled wire (b).

Fig. 7 Initial fouling rates as a function of the particle concentration for the annular probe (a)and for the coiled wire (b).

Fig. 8 Influence of the flow velocity on the asymptotic fouling resistance for the annular probe (a) and for the coiled wire (b).

Fig. 9 Influence of the heat flux on the asymptotic fouling resistance for the annular probe and for the coiled wire.

Fig. 10 Asymptotic fouling resistance for the annular probe as a function of the particle concentration and the bulk temperature.

TABLE 1 Range of System Parameters

System pressure	1 bar	$< p < 5.1$ bar
Bulk temperature	18°C	$< T_b <$ 61°C
Heat flux	0 W/m^2	$< \dot{q} <$ 375,000 W/m^2
Particle concentration	5 ppm	$< C <$ 400 ppm
Mass velocity in the annulus	10 kg/m^{2}s	$< \dot{m} <$ 442 kg/m^{2}s
Mass velocity past the coiled wire	3 kg/m^{2}s	$< \dot{m} <$ 353 kg/m^{2}s

TABLE 2 Dimensions of Heating Elements

Coiled Wire		Annular Probe	
Material	SS 410	Material	SS 316
Wire diameter	0.2 mm	Core diameter	10.7 mm
Wire length	125 mm	Annulus outer diameter	25.4 mm
Coil diameter	1.25 mm	Heated length	102.0 mm
Number of coils	25	Heated length to thermocouple location	78.0 mm
Duct cross-section	40 mm x 13 mm	Entrance length to thermocouple location	294.0 mm

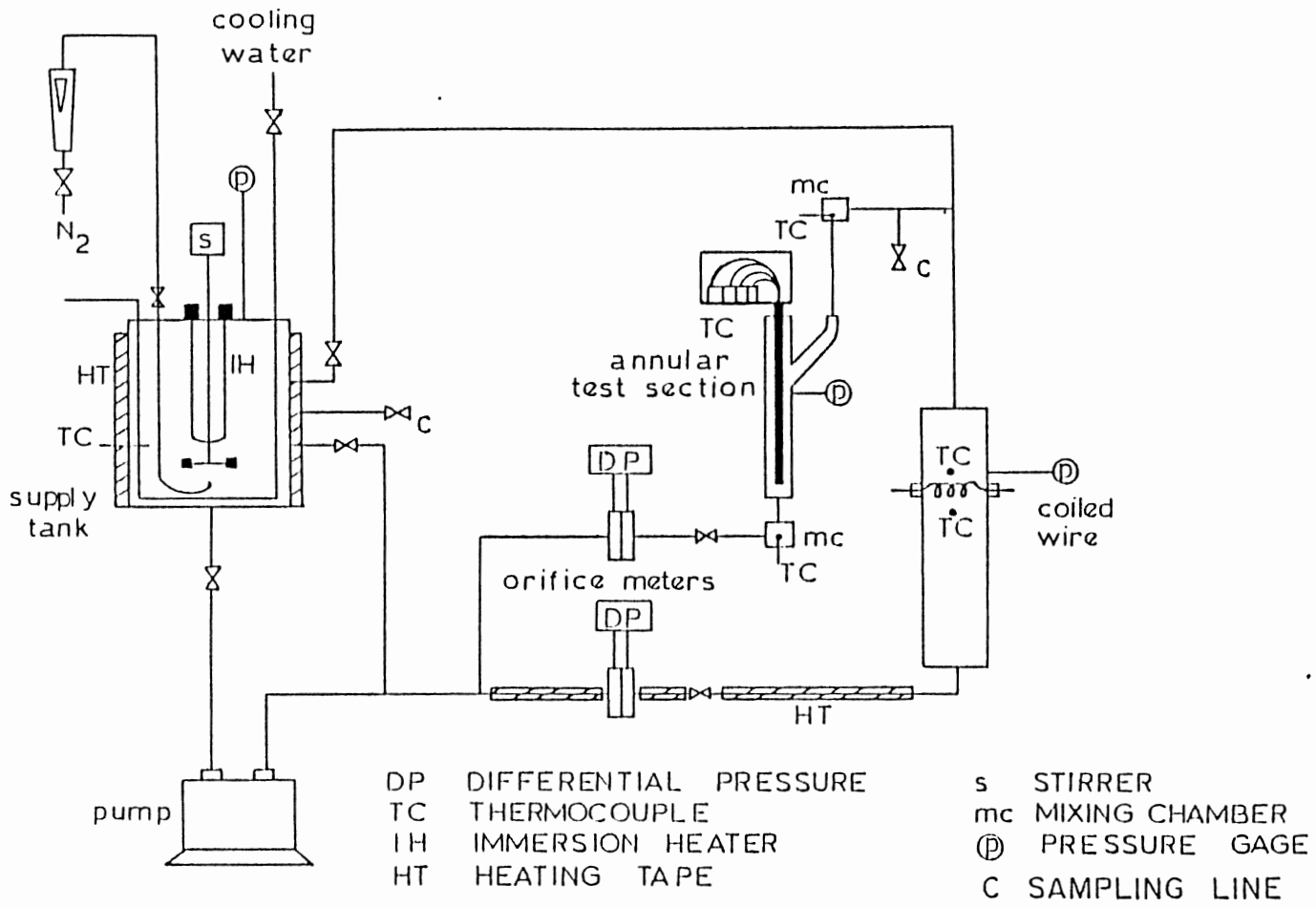
cooling
water
N2
S
HT
IH
TC
C
supply
tank
pump
mc
TC
C
TC
annular
test section
DP
orifice meters
mc
TC
DP
HT
TC
TC
coiled
wire
DP DIFFERENTIAL PRESSURE
TC THERMOCOUPLE
IH IMMERSION HEATER
HT HEATING TAPE
S STIRRER
mc MIXING CHAMBER
Ⓟ PRESSURE GAGE
C SAMPLING LINE

Fig. 1

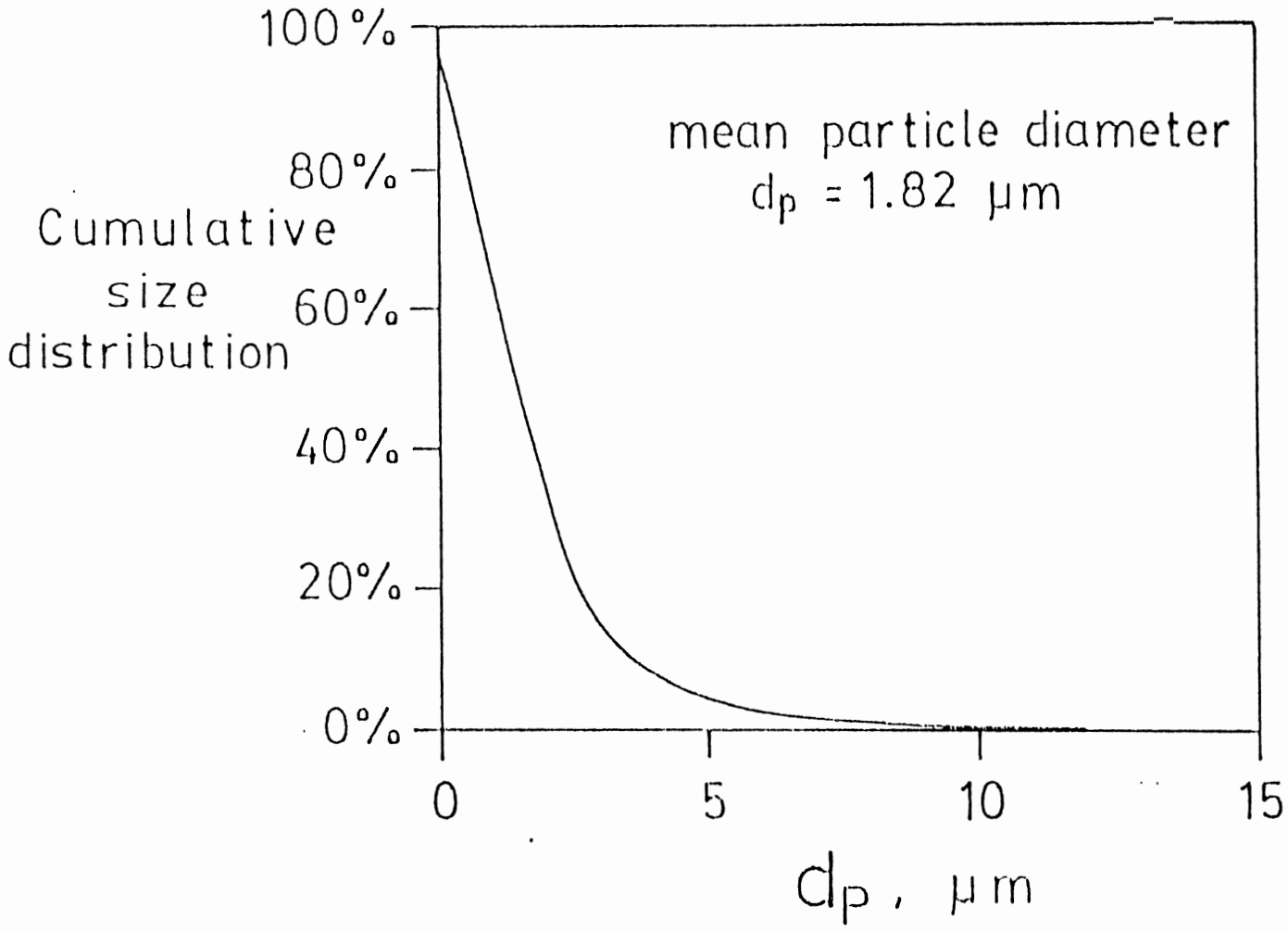
100 %
80 %
60 %
40 %
20 %
0 %
Cumulative size distribution
mean particle diameter
d_p = 1.82 µm
0
5
10
15
d_p , µm

Fig. 2

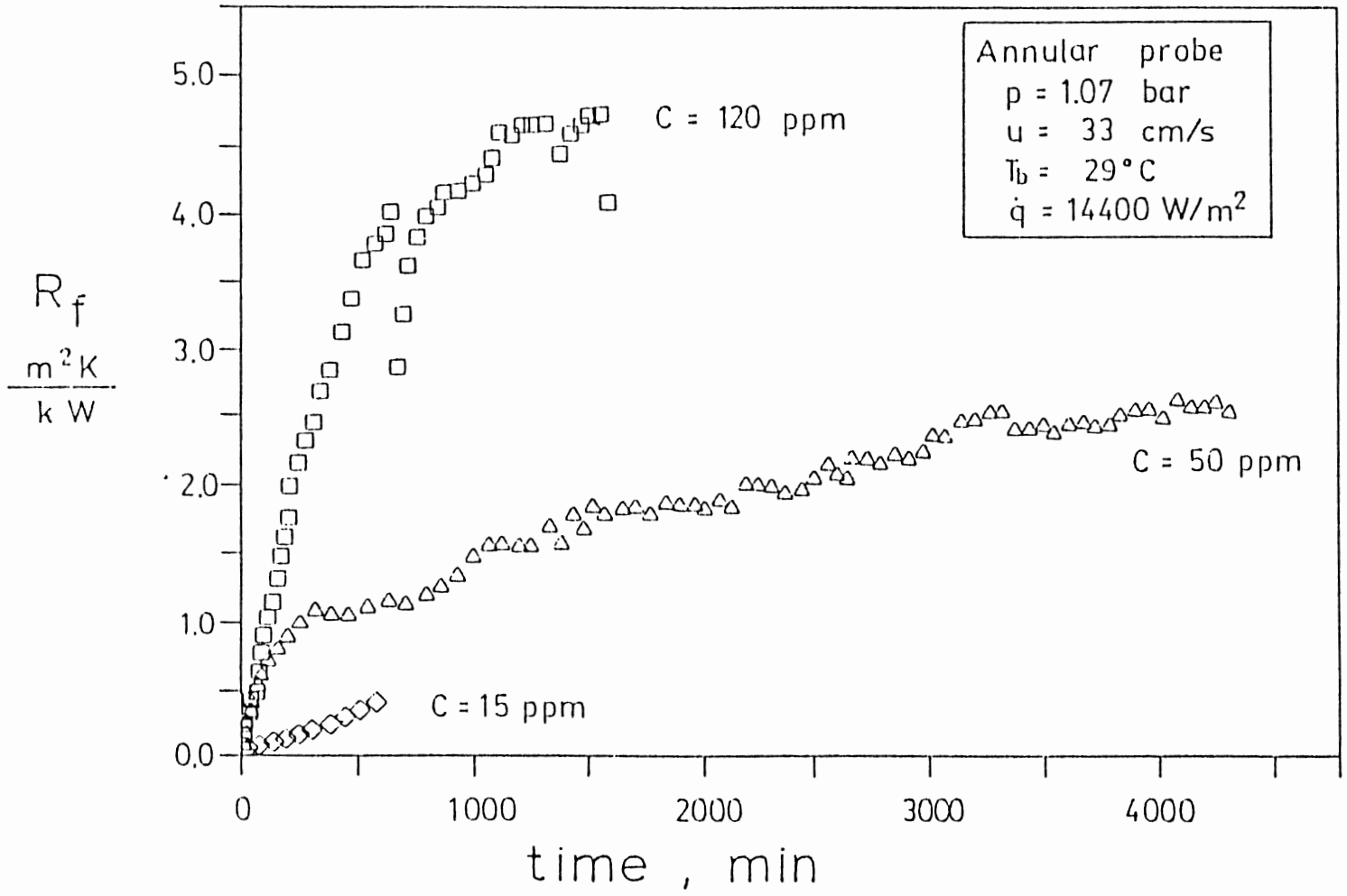
Annular probe
p = 1.07 bar
u = 33 cm/s
T_b = 29 °C
$\dot{q}$ = 14400 W/m²
C = 120 ppm
C = 50 ppm
C = 15 ppm
R_f
$\frac{m^2K}{kW}$
5.0
4.0
3.0
2.0
1.0
0.0
0
1000
2000
3000
4000
time , min

Fig. 3a

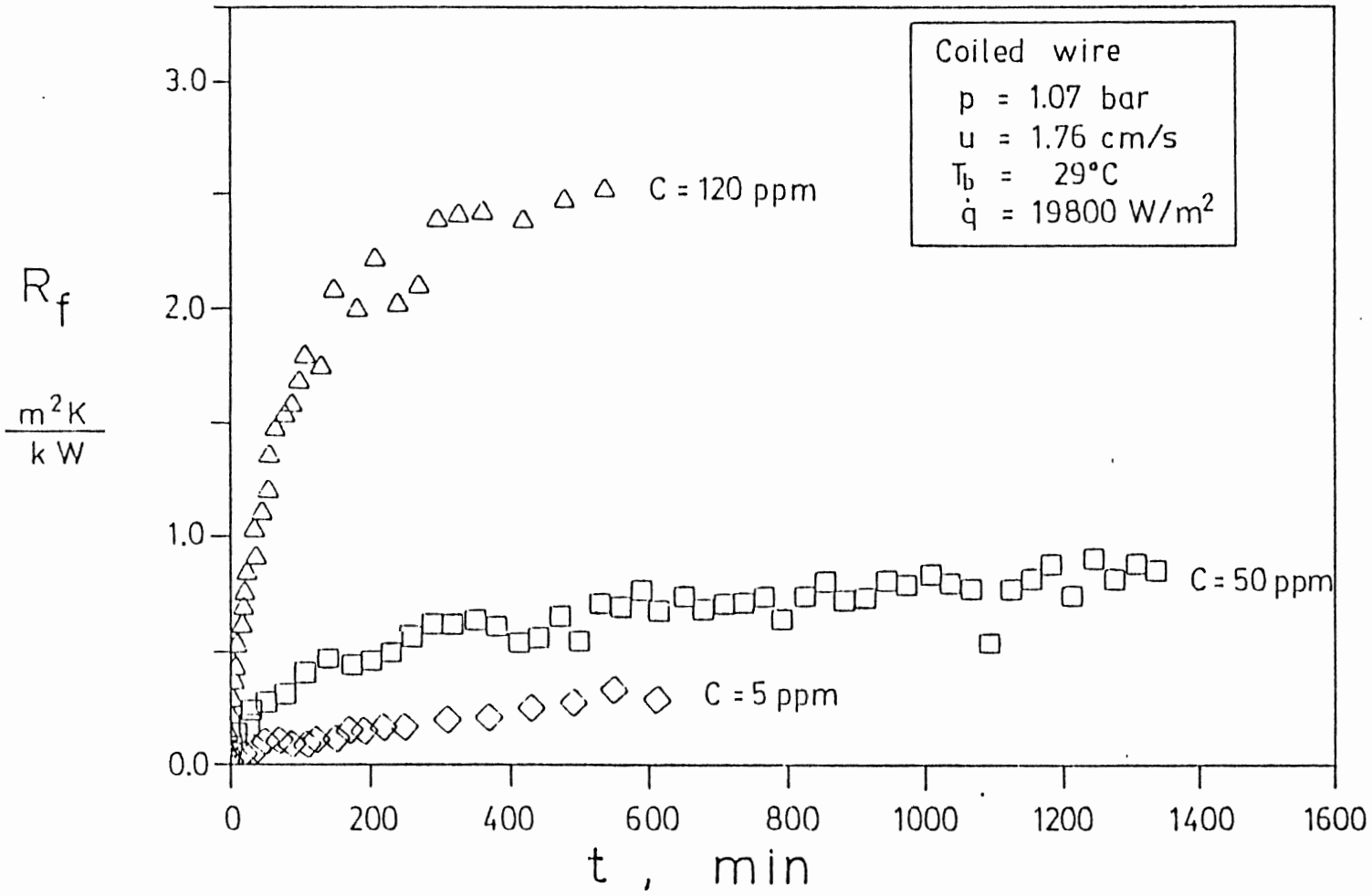
Coiled wire
p = 1.07 bar
u = 1.76 cm/s
T_b = 29°C
$\dot{q}$ = 19800 W/m²
C = 120 ppm
C = 50 ppm
C = 5 ppm
R_f
$\frac{m^2K}{kW}$
3.0
2.0
1.0
0.0
0
200
400
600
800
1000
1200
1400
1600
t , min

Fig 3b

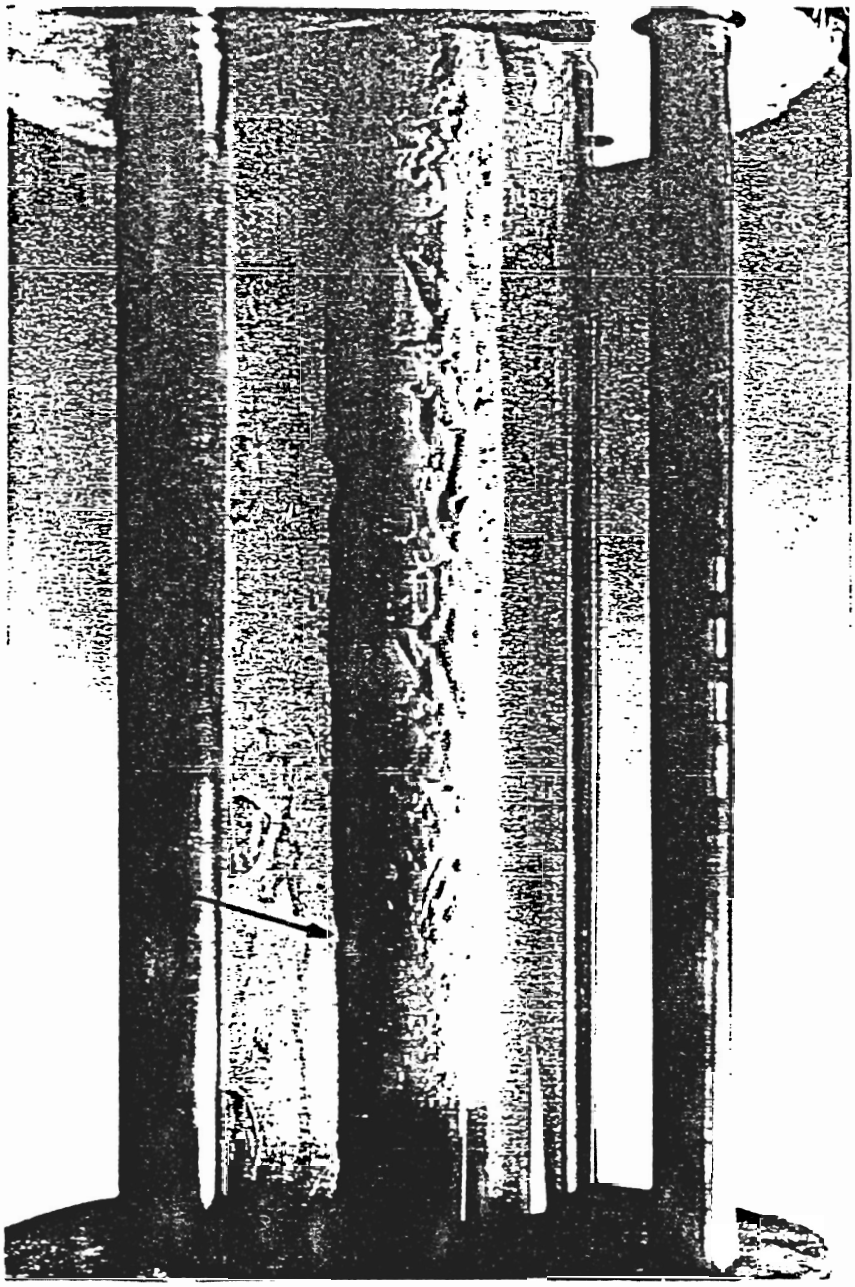

Fig. 4

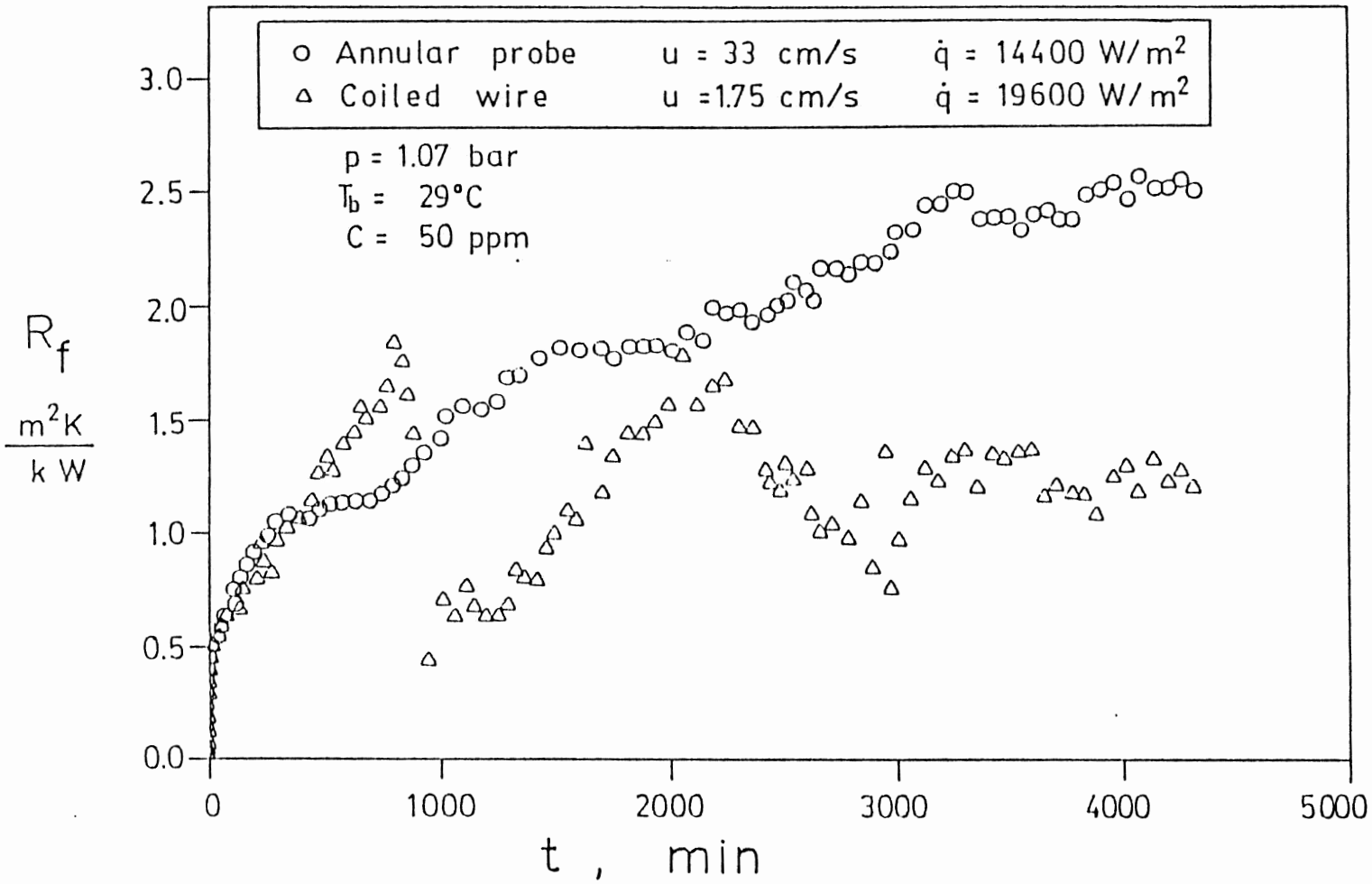
o Annular probe u = 33 cm/s q̇ = 14400 W/m²
Δ Coiled wire u = 1.75 cm/s q̇ = 19600 W/m²
p = 1.07 bar
T_b = 29°C
C = 50 ppm
R_f
m²K/kW
3.0
2.5
2.0
1.5
1.0
0.5
0.0
0
1000
2000
3000
4000
5000
t , min

Fig. 5

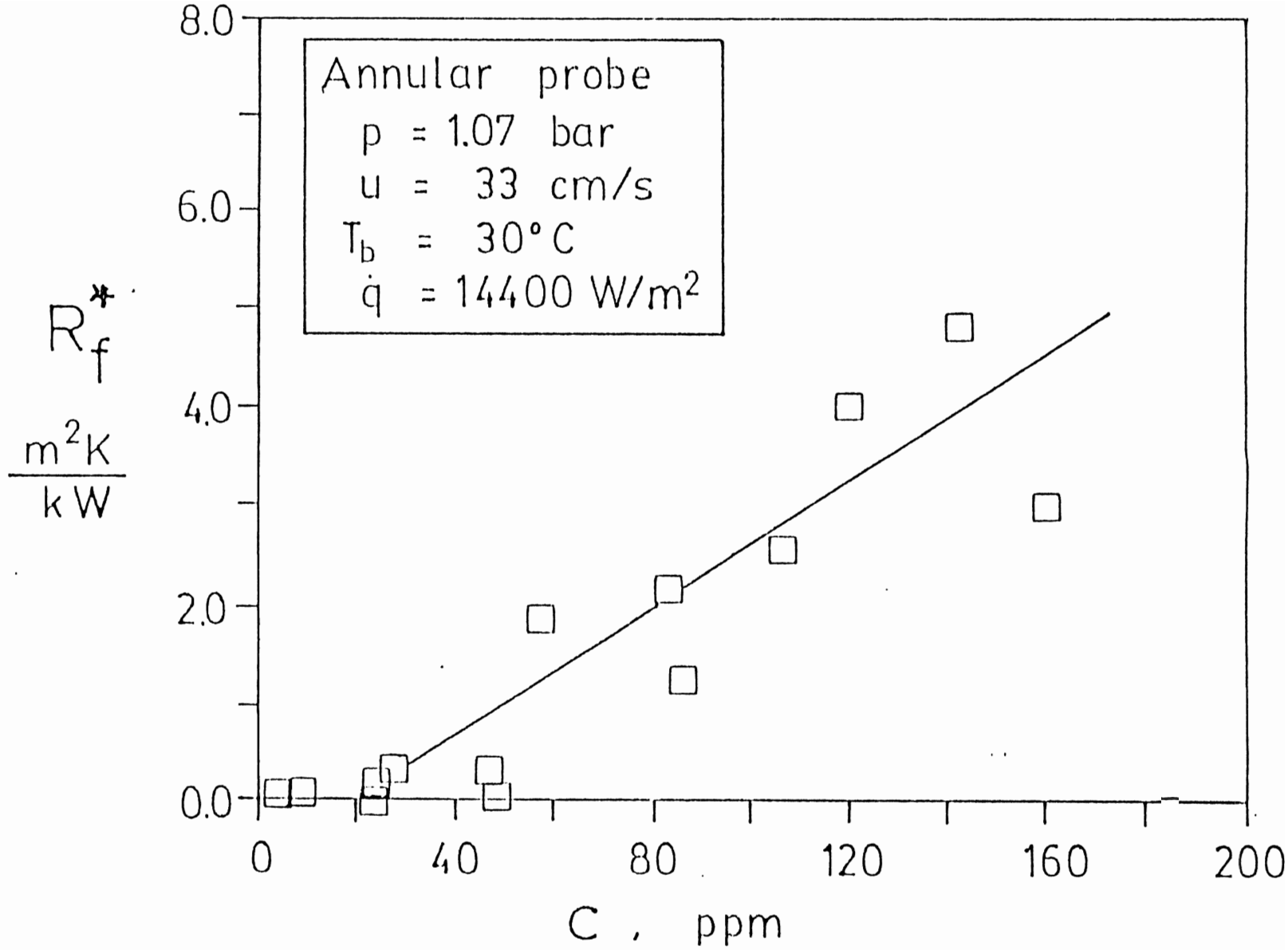
Annular probe
p = 1.07 bar
u = 33 cm/s
T_b = 30° C
$\dot{q}$ = 14400 W/m²
R_f^*
$\frac{m^2K}{kW}$
8.0
6.0
4.0
2.0
0.0
0
40
80
120
160
200
C , ppm

Fig.6a

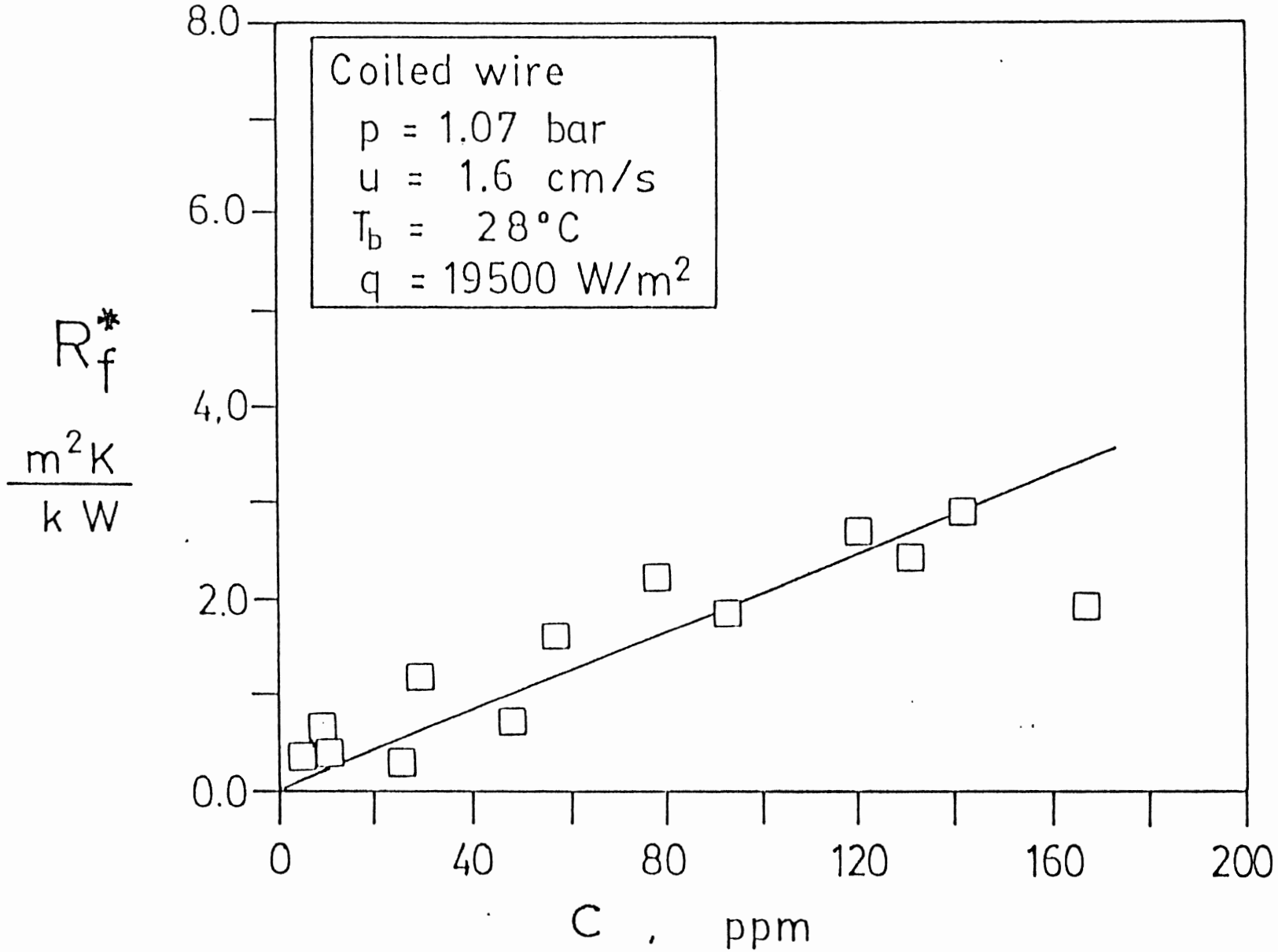
Coiled wire
p = 1.07 bar
u = 1.6 cm/s
T_b = 28°C
q = 19500 W/m²
R_f^*
$\frac{m^2K}{kW}$
8.0
6.0
4.0
2.0
0.0
0
40
80
120
160
200
C , ppm

Fig. 6b

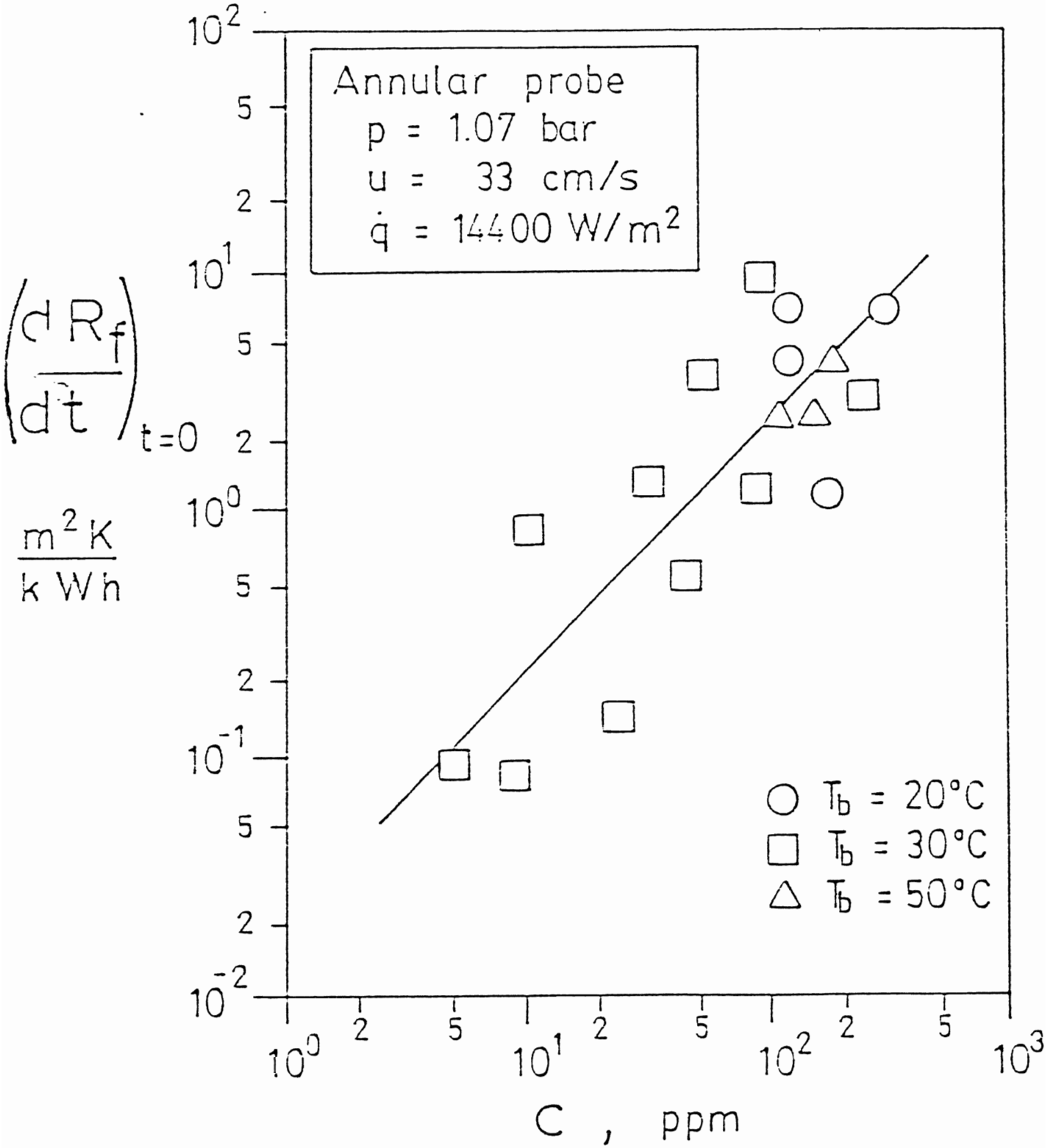
Annular probe
p = 1.07 bar
u = 33 cm/s
q̇ = 14400 W/m²
$\left(\frac{dR_f}{dt}\right)_{t=0}$
m²K / kWh
10^2
5
2
10^1
5
2
10^0
5
2
10^{-1}
5
2
10^{-2}
10^0
2
5
10^1
2
5
10^2
2
5
10^3
C , ppm
○ T_b = 20°C
□ T_b = 30°C
△ T_b = 50°C

Fig. 7a

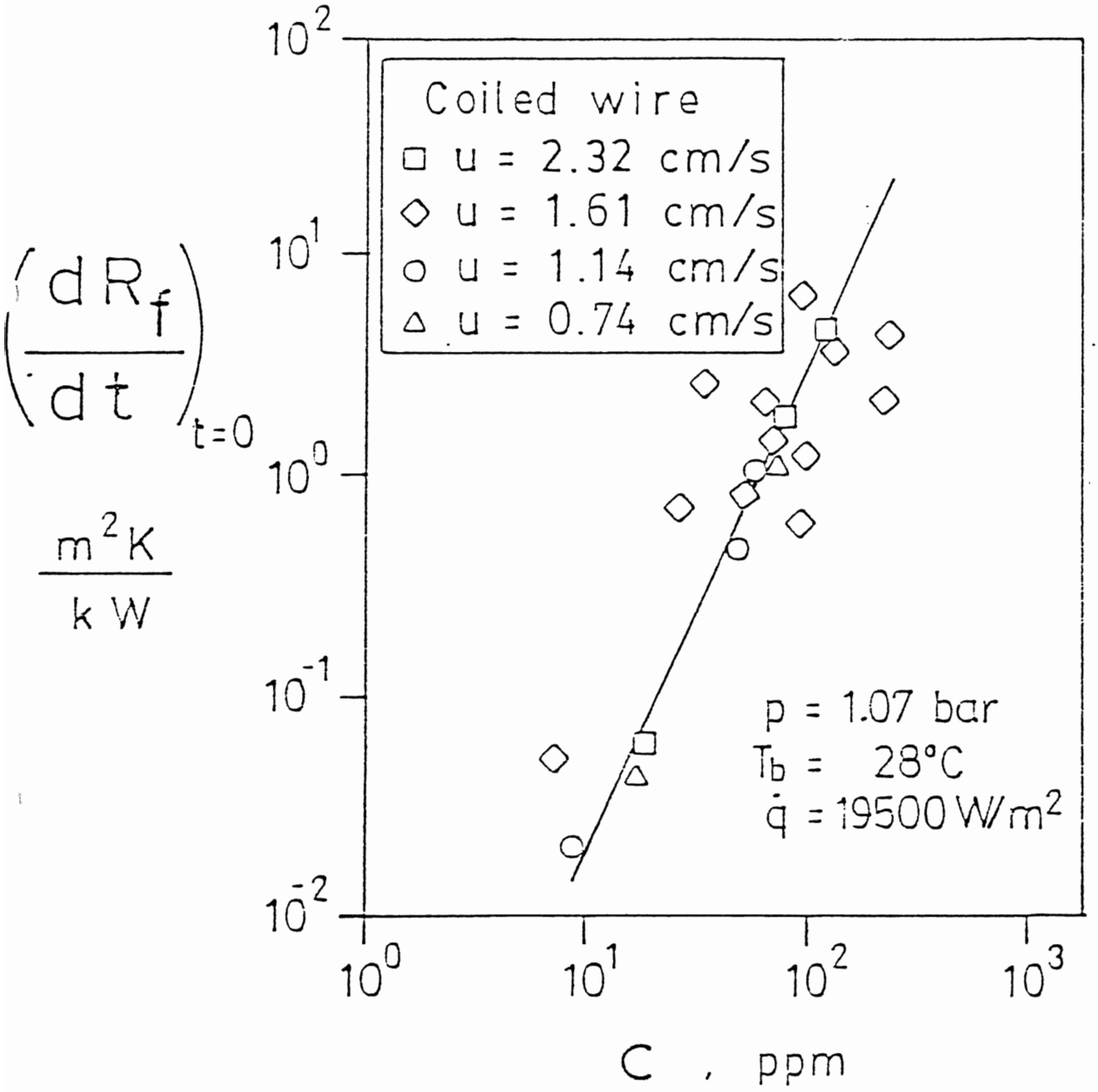
Coiled wire
□ u = 2.32 cm/s
◇ u = 1.61 cm/s
○ u = 1.14 cm/s
△ u = 0.74 cm/s
p = 1.07 bar
T_b = 28°C
$\dot{q}$ = 19500 W/m²
$\left(\frac{dR_f}{dt}\right)_{t=0}$
$\frac{m^2K}{kW}$
10^2
10^1
10^0
10^{-1}
10^{-2}
10^0
10^1
10^2
10^3
C , ppm

Fig. 7b

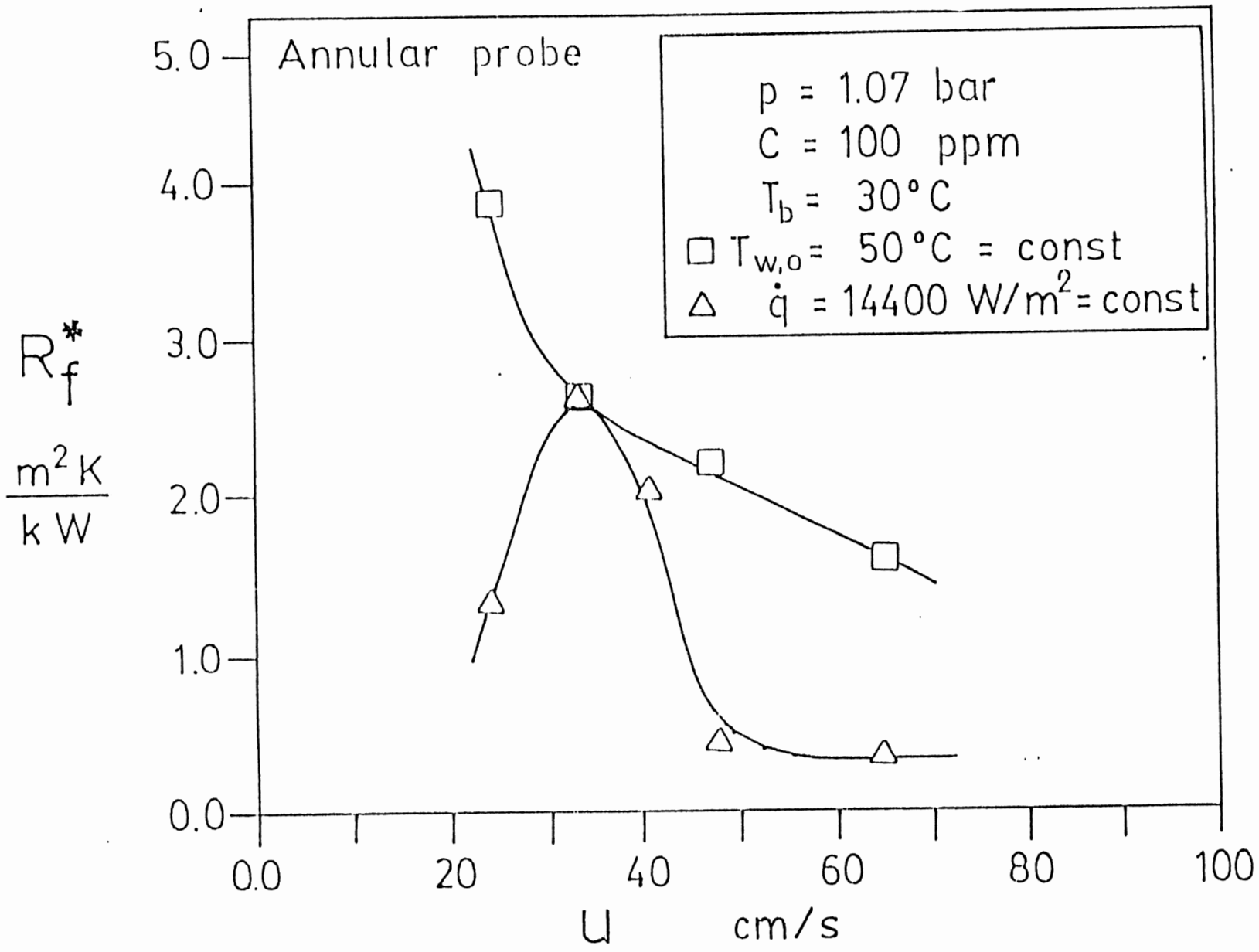
Annular probe
p = 1.07 bar
C = 100 ppm
T_b = 30 °C
□ $T_{w,o}$ = 50 °C = const
△ $\dot{q}$ = 14400 W/m² = const
R_f^*
$\frac{m^2 K}{kW}$
5.0
4.0
3.0
2.0
1.0
0.0
0.0
20
40
60
80
100
U cm/s

Fig. 1

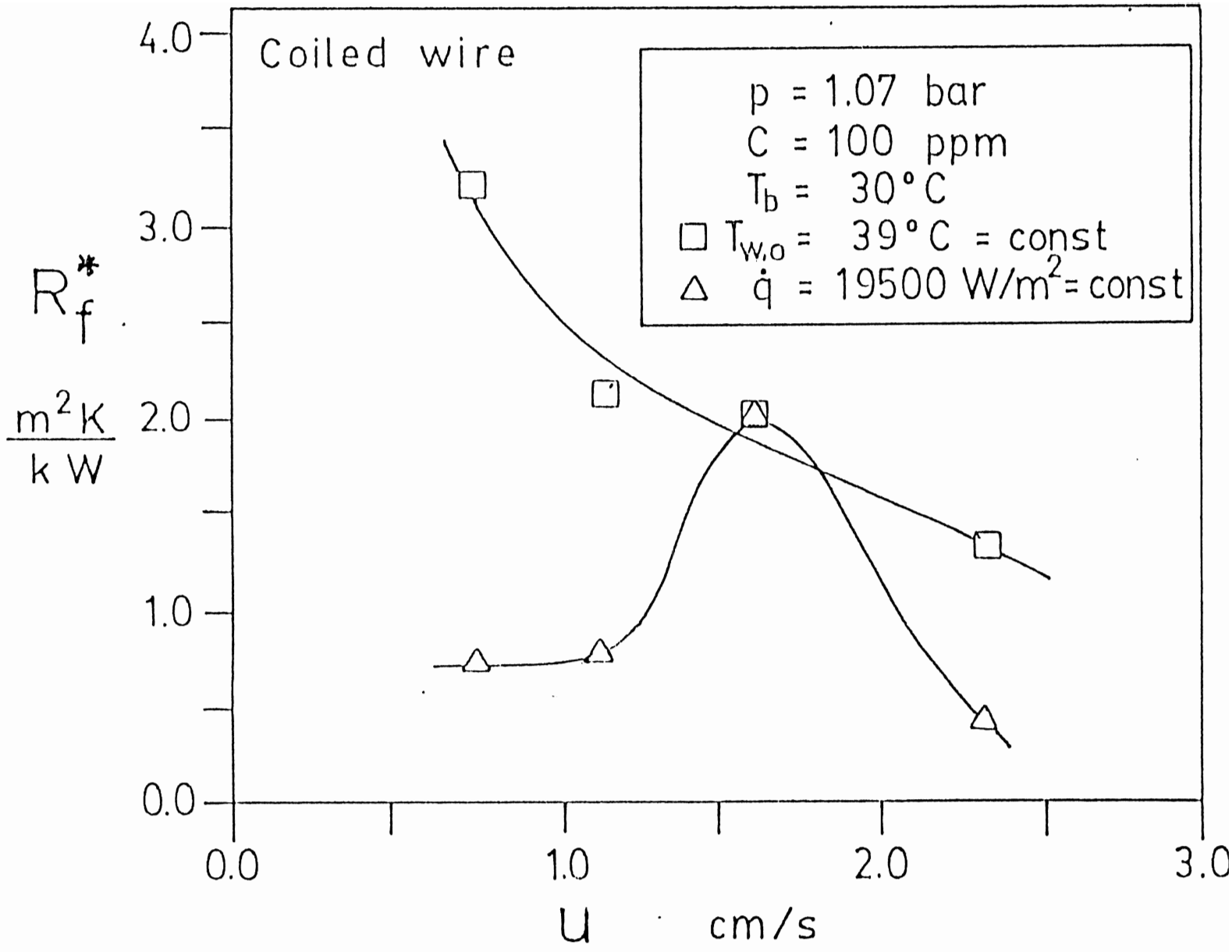
Coiled wire
p = 1.07 bar
C = 100 ppm
T_b = 30°C
□ $T_{w,o}$ = 39°C = const
△ $\dot{q}$ = 19500 W/m² = const
R_f^*
$\frac{m^2K}{kW}$
4.0
3.0
2.0
1.0
0.0
0.0
1.0
2.0
3.0
U cm/s

Fig. 8b

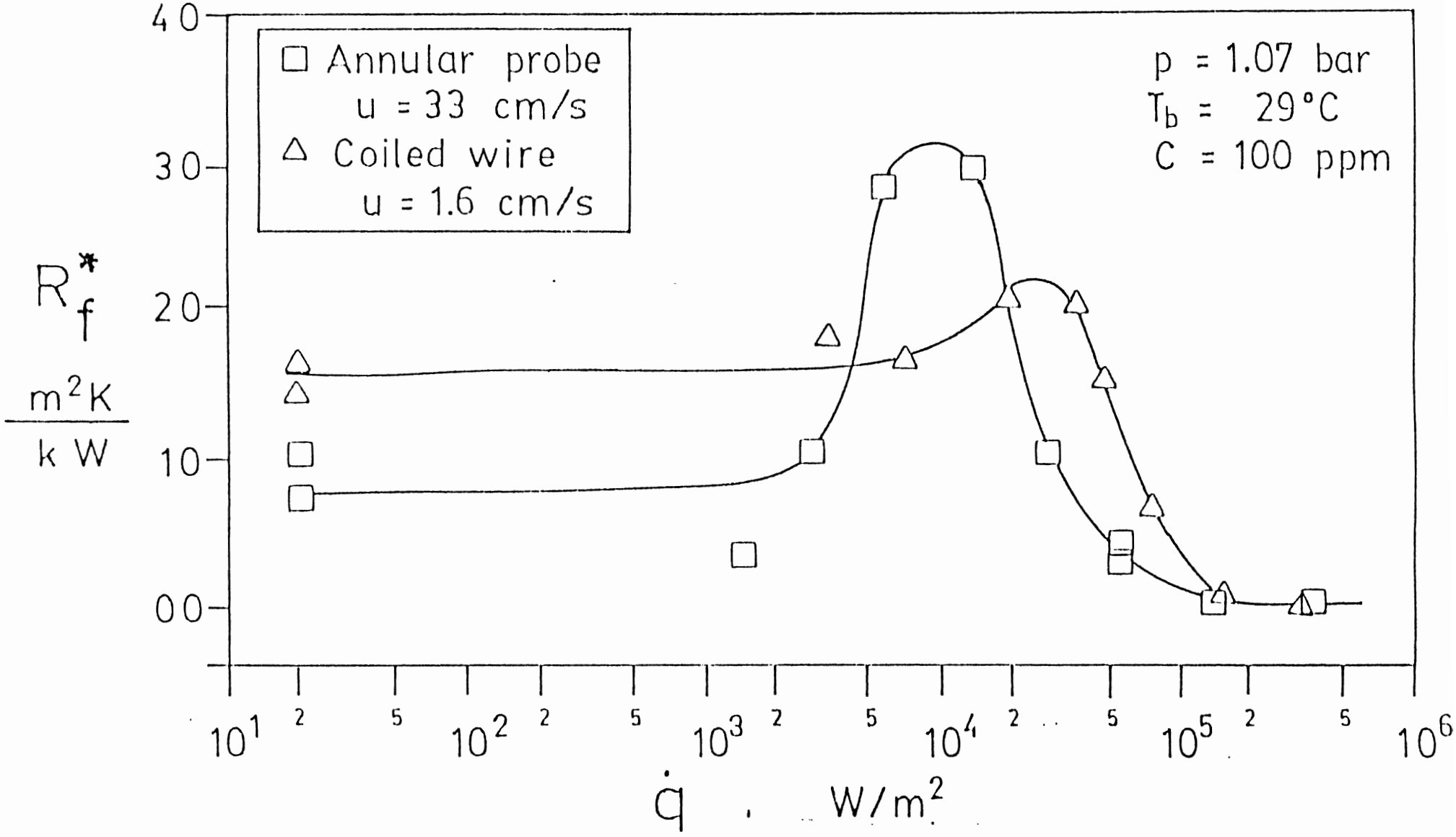
Annular probe
u = 33 cm/s
Coiled wire
u = 1.6 cm/s
p = 1.07 bar
T_b = 29°C
C = 100 ppm
R_f^*
$\frac{m^2K}{kW}$
40
30
20
10
00
10^1
2
5
10^2
2
5
10^3
2
5
10^4
2
5
10^5
2
5
10^6
$\dot{q}$. W/m²

Fig 9

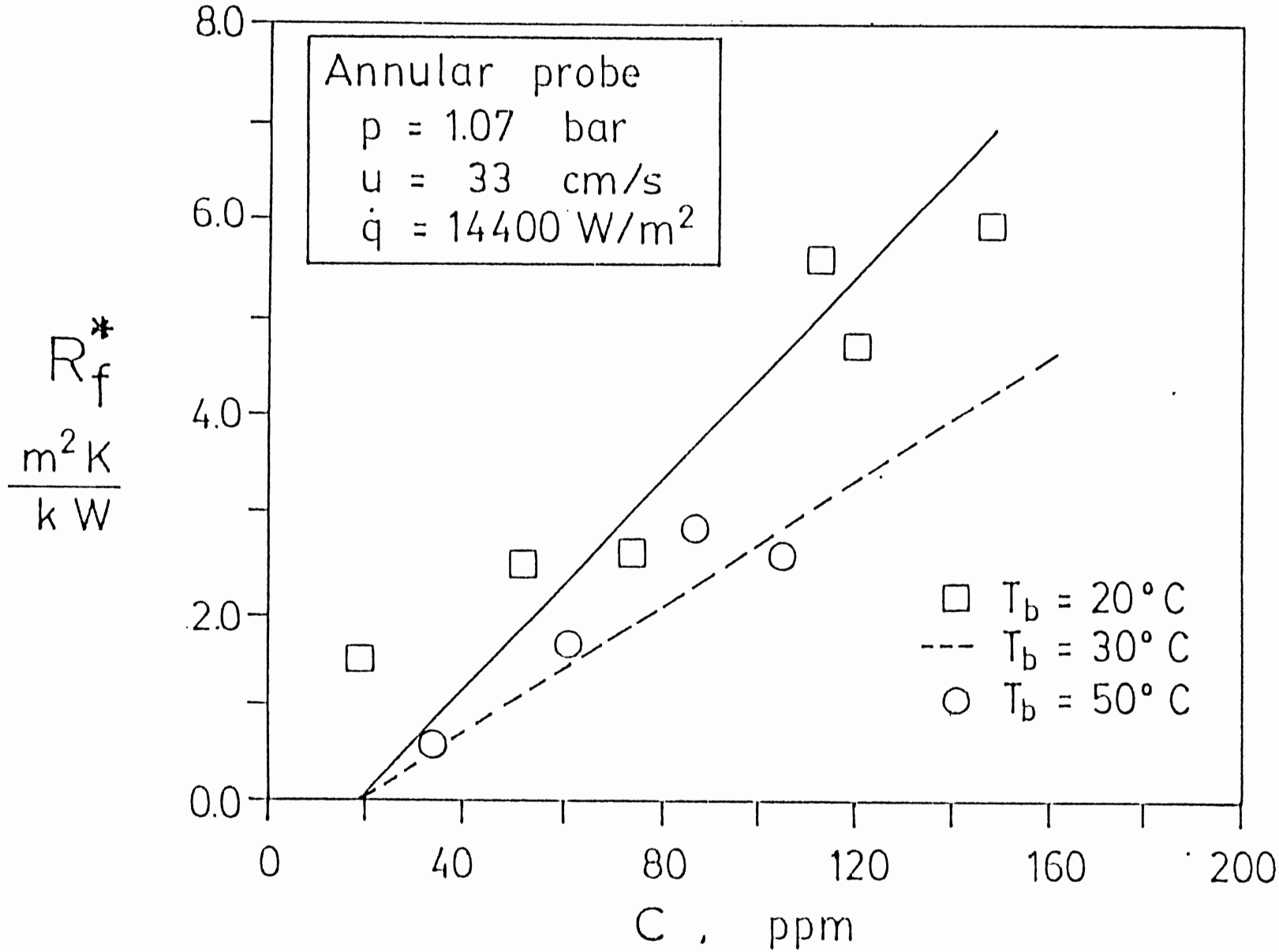
Annular probe
p = 1.07 bar
u = 33 cm/s
q̇ = 14400 W/m²
R_f^*
$\frac{m^2 K}{kW}$
8.0
6.0
4.0
2.0
0.0
0
40
80
120
160
200
C , ppm
T_b = 20° C
T_b = 30° C
T_b = 50° C

Fig. 10